2026 IEEE Transportation Electrification Conference & Expo (ITEC) & Electric Aircraft Technologies Symposium (EATS) (ITEC+EATS) | 979-8-3315-8773-4/26/$31.00 ©2026 IEEE | DOI: 10.1109/ITECEATS66641.2026.11592818

Universal High-Frequency Modeling Methods of Electrical Machines Using Impedance Fitting

1st Hujun Peng
Institute of Electrical Machines (IEM)
RWTH Aachen University
Aachen, Germany
hujun.peng@iem.rwth-aachen.de

2nd Yue Yu
Institute of Electrical Machines (IEM)
RWTH Aachen University
Aachen, Germany
yue.yu@iem.rwth-aachen.de

3rd Nora Leuning
Institute of Electrical Machines (IEM)
RWTH Aachen University
Aachen, Germany
nora.leuning@iem.rwth-aachen.de

4th Simon Steentjes
Institute of Electrical Machines (IEM)
RWTH Aachen University
Aachen, Germany
simon.steentjes@iem.rwth-aachen.de

***Abstract*—Wide-bandgap (WBG) semiconductor power devices, such as SiC and GaN MOSFETs, are increasingly adopted in electrical drive systems due to their superior efficiency and power density. However, their high switching frequencies introduce significant electromagnetic interference (EMI), leading to overvoltage oscillations at machine terminals. To quantitatively analyze EMI induced by power module switching in electrical drives, this paper proposes a universal high-frequency grey-box model for machine windings, incorporating frequency-dependent impedance characteristics and mutual inductance effects between phases. The model is parameterized using impedance measurements and validated through both frequency-domain and time-domain experiments. Frequency-domain validation confirms that the model accurately reproduces impedance spectra across a broad frequency range up to 10 MHz, making it applicable to various machine types. Time-domain validation further demonstrates its capability to predict transient oscillations in common-mode (CM) voltage at the machine terminals. These findings highlight the model's effectiveness in capturing transient behaviors across diverse machine and winding configurations, providing a valuable tool for optimizing electrical machine insulation design and mitigating voltage stress.**

***Index Terms*—Electrical machine, Hairpin winding, High-frequency modeling, Insulation system, Overvoltage.**

I. Introduction

Wide-bandgap (WBG) semiconductor power devices, such as SiC and GaN MOSFETs, are increasingly integrated into electrical drive systems due to their superior performance in reducing torque and speed ripple while minimizing power losses under various operating conditions compared to conventional IGBT-based solutions [1]. However, the high switching frequency and rapid voltage slew rates of WBG devices introduce significant challenges, particularly in the form of overvoltage oscillations at machine terminals during switching events [2]. When electrical machines are connected via long cables, the peak voltage at the terminals can reach up to twice the DC-link voltage [3], imposing substantial stress on the insulation system. Ensuring compliance with IEC 60034-18-41 [4] is therefore crucial during the design phase. A common mitigation strategy involves overdesigning the insulation system; however, this conservative approach can be avoided by employing an accurate high-frequency model of machine windings, enabling precise assessment of voltage stress at the machine terminals. High-frequency modeling approaches can be broadly categorized into two types: white-box models and grey-box models. White-box models, as demonstrated in [5], [6], rely on equivalent electrical circuits derived from finite element analysis (FEA). While these models provide high accuracy by incorporating detailed material properties and geometric data, their application is often constrained by the high computational cost associated with non-linearity and frequency-dependent permeability, particularly at frequencies in the megahertz range. In contrast, grey-box models are widely used for existing electrical components and are parameterized based on impedance measurements. Rather than explicitly modeling internal structures, these models capture the external electrical behavior resulting from internal interactions. For instance, the study in [7] proposes a high-frequency grey-box model for an open-winding motor. In contrast, [8] develops separate models for common-mode (CM) and differential-mode (DM) impedance. However, these models do not fully account for phase-to-phase variations and lack comprehensive time-domain validation. Additionally, a coil-based model proposed in [9] specifically targets hairpin stator windings but remains limited to a particular machine type, restricting its broader applicability. Despite these advancements, a universal high-frequency winding model that accounts for internal interactions and is applicable across various machine topologies has yet to be established. This paper addresses this gap by presenting a general high-frequency grey-box machine model capable of accurately characterizing frequency-dependent impedance and mutual inductance effects across different machine types.

To bridge the gap in high-frequency modeling, this work makes the following contributions:

- Development of a universal grey-box model: A high-

frequency grey-box model applicable to various types of electrical machines is proposed, integrating frequency-dependent impedance characteristics and mutual interactions among different phases.
- Comprehensive frequency-domain validation: The proposed model is validated across various machine types, accurately capturing impedance behavior up to $10\,\mathrm{MHz}$.
- Time-domain validation and transient analysis: The model is further validated using measurements from a test bench of an operating PMSM, demonstrating its accuracy in overvoltage prediction and its capability to capture transient behaviors at machine terminals under different operating conditions.

The remainder of this paper is organized as follows: Section II presents the high-frequency modeling approach for electrical machines based on impedance spectra. Section III validates the general applicability of the proposed model across different machine types in the frequency domain. Section IV describes the time-domain validation using measurements obtained from a test bench. Finally, Section V concludes the study and discusses potential directions for future research.

II. Universal Grey-box Model

A. *Impedance Measurement*

The transient behavior at machine terminals is influenced by the frequency-dependent properties of the windings, including skin effect, proximity effect, and parasitic capacitance among internal machine components. To analyze the external manifestations of these effects, the proposed model is implemented based on impedance measurements at the machine terminals.

In this study, impedance spectra are measured using a Keysight E4990A impedance analyzer under different terminal connection configurations, covering a frequency range from $100\,\mathrm{Hz}$ to $10\,\mathrm{MHz}$. This range extends approximately 100 times beyond the upper switching frequency limit of SiC-based power devices, ensuring comprehensive high-frequency characterization. The measured impedance data are classified into two categories based on different electromagnetic interference (EMI) propagation paths:

- Common-Mode (CM) impedance (phase-to-housing impedance): Reflects the overall characteristics of the machine insulation systems.
- Differential-Mode (DM) impedance, including phase-to-phase and phase-to-phases impedance.

Table I summarizes the measurement configurations based on the three-phase windings, labeled as U, V, and W. These

TABLE I
Terminal connection topologies for impedance spectrum measurement of electrical machines.

Category	Example	**Measurement between** one phase terminal and
phase-to-housing	U-GND	machine housing
phase-to-phase	U-V	another phase-terminal
phase-to-phases	U-VW	the other shorted phases

pre-measurements serve as a standard procedure to guide the modeling process and will later be utilized for parameterization via curve fitting. Fig. 1 presents an example of common-mode (CM) and differential-mode (DM) impedance measurements of the winding. For the CM impedance spectrum shown in Fig. 1a, the low-frequency region (below $100\,\mathrm{kHz}$) exhibits a significantly high impedance magnitude, with a phase angle maintained at approximately $-90°$, indicating the capacitive nature of the insulation system between the windings and the machine housing. As the frequency increases, inductive characteristics become dominant, introducing resonance points in the high-frequency range below $1\,\mathrm{MHz}$. In Fig. 1b, the winding DM-impedance initially exhibits inductive behavior up to approximately $500\,\mathrm{kHz}$. Due to the skin effect and proximity effect of conductors, the impedance amplitude increases with frequency. Beyond this point, capacitive effects along the winding direction become more pronounced, attributed to the influence of parasitic capacitance. These frequency-dependent characteristics are consistently observed across various machine types and must be accounted for in the development of a universal high-frequency model for electrical machines.

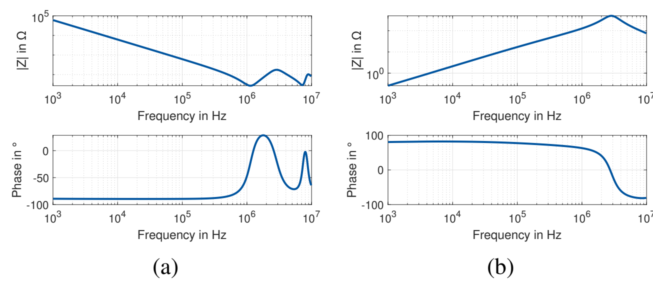

Fig. 1. Examples of CM and DM impedance measurement of a PMSM stator winding: (a) U-to-housing, (b) U-V.

B. *Universal Model Structure*

Fig. 2a illustrates the structural overview of the proposed grey-box model for three-phase electrical machines. This approach decomposes the model into several branches, each representing the corresponding frequency response behavior within a different frequency interval. As the number of resonance points increases across the frequency spectrum, the complexity of the modeled machine's frequency response also increases, necessitating additional branches.

The modeling focus is first on the blue-highlighted blocks in Fig. 2a, which capture the inductive behavior of conductors through a two-segment RL-ladder network structure, as detailed in Fig. 2b. Segment 'Part A' consists of a four-layer RL-ladder network to simulate the influence of the skin effect. Segment 'Part B' considers the proximity effect among phases using a three-layer RL-ladder network, incorporating mutual inductance coupling between windings of different phases. This inductive coupling among the U, V, and W phases is constrained within the same branch and its corresponding RL layers to balance model complexity and accuracy in capturing frequency-dependent effects. This design enables a relative decoupling of the skin and proximity effects based

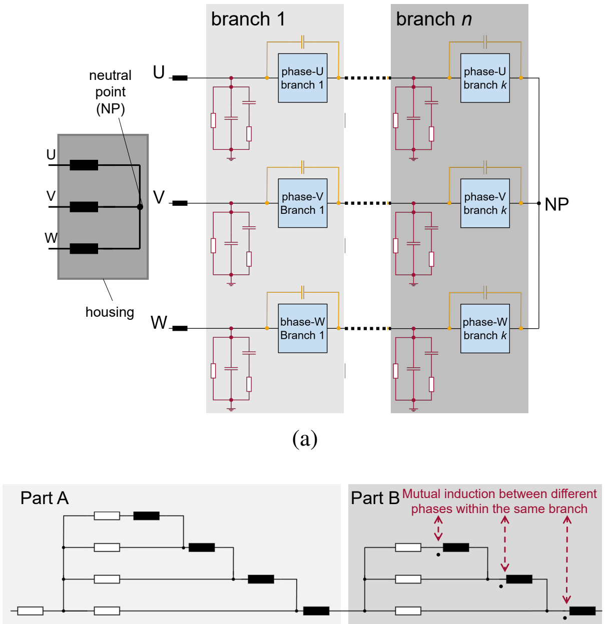

(a)

(b)

Fig. 2. Grey-box model structure: (a) structural overview, (b) Model details accounting for skin and proximity effect.

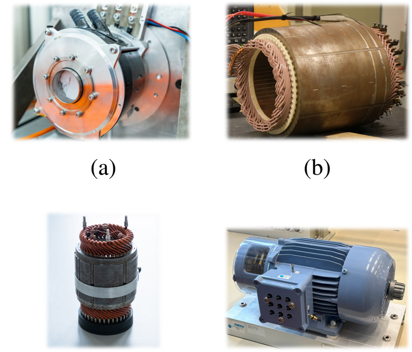

(a) (b)

(c) (d)

Fig. 3. Four types of electrical machines used for high-frequency modeling: (a) IPMSM, (b) IM, (c) SPMSM, (d) DFIM.

TABLE II
FOUR TYPES OF ELECTRICAL MACHINES USED FOR MODELING.

Machine ID	Machine type	Winding type
1	IPMSM	Single-tooth
2	IM	Hairpin
3	SPMSM	Hairpin
4	DFIM	Random Winding

on their distinct physical origins. Regarding the modeling of the insulation system between phase and housing within each branch, the leftmost resistor, with a significantly high resistance value, represents the DC resistance of the insulation layer. At the same time, the central capacitor models the parasitic capacitance between the windings and the housing. An RC network on the right side is introduced to describe dielectric losses, which become more pronounced at higher frequencies.

The modular structure of this model allows its complexity to be adapted based on the spectral characteristics of the winding under study. It is not constrained by motor or winding type. Regarding the capacitance between adjacent wires within the same phase, another capacitor is used for modeling this effect. In the next section, the applicability of the proposed model is validated across different types of motor windings.

III. Validation of Model Applicability in Frequency Domain

Using the approach described in Section II, the windings of four machines with varying types and geometric sizes are modeled. A summary of the winding details is provided in Table II, which includes the following machine types: interior permanent magnet synchronous machine (IPMSM), induction machine (IM), surface-mounted permanent magnet synchronous machine (SPMSM), and doubly-fed induction machine (DFIM). The parameterization processes are implemented using an optimization algorithm.

The parameterization process is performed using a curve-fitting algorithm from our previous work [10]. Figures 4 and 5 illustrate a comparative analysis of the modeled and measured impedance spectra for both CM and DM across the four machine types. The model demonstrates high accuracy up to several megahertz in the frequency domain, which is nearly 100 times higher than the upper limit of the WBG device switching frequency. This highlights its capability to precisely capture voltage oscillations at the machine terminals induced by the WBG device.

Considering the equivalent electric circuits shown in Fig. 2, the high-frequency model is constructed using linear electrical elements. Consequently, each modeled impedance spectrum can be interpreted as a Frequency Response Function (FRF), where a hypothetical current excitation signal serves as the input and the resulting voltage signal as the output. The measured impedance spectrum represents the actual FRF of the system.

To evaluate the impedance model in the frequency domain, the Ordinary Coherence between the Power Spectral Densities (PSDs) of the modeled and measured spectra is computed based on the topologies listed in Table I. This approach is inspired by FRF comparison methods commonly used in vibration analysis, as detailed in [11]. An Ordinary Coherence value close to 1 indicates a strong linear correlation between the two FRFs. In this study, such a value confirms that the high-frequency model accurately captures the winding's frequency response characteristics.

Tab. III presents the average Ordinary Coherence between modeled and measured impedance spectra across all topologies for modeled windings, within the frequency range from 1 kHz to 10 MHz. An overall value higher than 0.96 is achieved for various winding types and machine types. The general applicability of this high-frequency model is validated in the frequency domain.

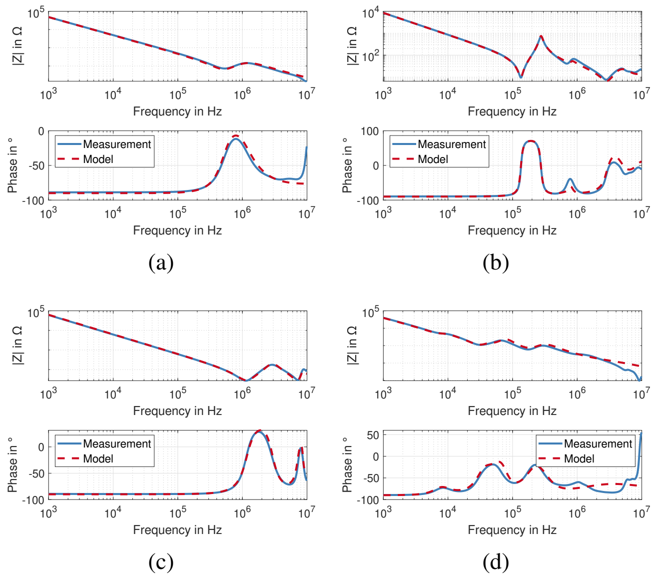

Fig. 4. Illustrative comparison of measured and modeled CM impedance spectra across various electrical machines: (a) the IPMSM, (b) the IM, (c) the SPMSM, (d) the DFIM.

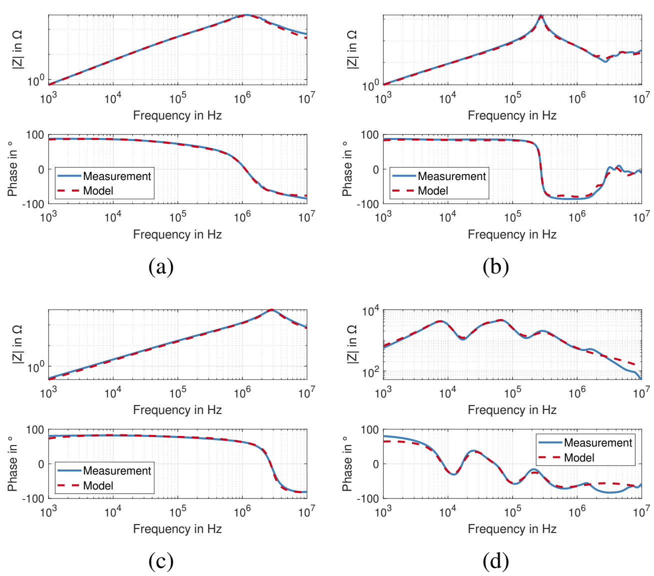

Fig. 5. Illustrative comparison of measured and modeled DM impedance spectra across various electrical machines: (a) the IPMSM, (b) the IM, (c) the SPMSM, (d) the DFIM.

TABLE III
SUMMARY OF THE AVERAGE ORDINARY COHERENCE BETWEEN MODELED AND MEASURED IMPEDANCE SPECTRA ACROSS ALL TOPOLOGIES FOR MACHINE WINDINGS.

Machine type	Winding type	Ordinary Coherence
IPMSM	Single-tooth	0.9661
IM	Hairpin	0.9697
SPMSM	Hairpin	0.9961
DFIG	Random Winding	0.9829

IV. MODEL VALIDATION IN TIME DOMAIN

The IPMSM depicted in Fig. 3a is selected for time-domain validation of the high-frequency model using measurements

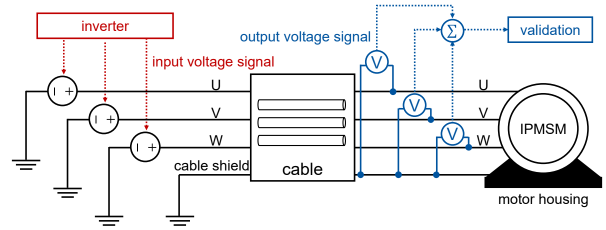

Fig. 6. Test bench for time-domain validation, measuring three phase-to-housing voltages at the motor terminals to compute the common-mode voltage.

from the test bench. The test bench setup, shown in Fig. 6, is designed for this validation. The IPMSM is powered through a shielded cable set by an inverter integrated with an SiC power module, which generates the voltage signal used as the simulation input. The high-frequency model of the IPMSM is coupled with a validated cable model to enhance accuracy.

To evaluate the model's capability in capturing voltage oscillations at the machine terminals, the common-mode voltage signal on the IPMSM side is computed and compared with corresponding simulation results. The common-mode voltage is obtained by summing the three phase-to-housing voltage signals at the machine terminals. The validation is performed under various switching frequencies $f_{\mathbf{sw}}$ and machine rotation speeds n in no-load conditions.

Figure 7 presents representative results of the time-domain validation. Experimental findings indicate that within the switching frequency range of $8\,\mathrm{kHz}$ to $32\,\mathrm{kHz}$, the high-frequency model effectively captures the terminal voltage oscillation behavior across various machine operating speeds. Thereby, the voltage oscillation profile exhibits high irregularity due to parasitic EMI effects within the switching circuit and the influence of the cable, and the oscillation period remains extremely short, typically within a few hundred nanoseconds. Switching events at the IPMSM terminals is calculated. Figure 8 presents a statistical analysis of these errors. Overall, the high-frequency model maintains a prediction error within $10\,\%$, with an average relative error of $8.31\,\%$ for the CM voltage peak. These results validate the model's accuracy in simulating terminal voltage oscillations in the time domain. The model effectively accounts for parasitic EMI effects introduced by WBG power devices in electric drive systems, accurately capturing the terminal voltage profile across various operating speeds and switching frequencies. Furthermore, its ability to provide reliable peak voltage predictions makes it a valuable tool for optimizing motor insulation system design and EMI filter development.

V. CONCLUSIONS AND OUTLOOKS

This study presents a universal high-frequency grey-box model for various electric machines, validated through frequency- and time-domain experiments. The model effectively captures frequency response characteristics from $1\,\mathrm{kHz}$ to $10\,\mathrm{MHz}$ and accurately predicts transient voltage oscillations at machine terminals under various operating condi-

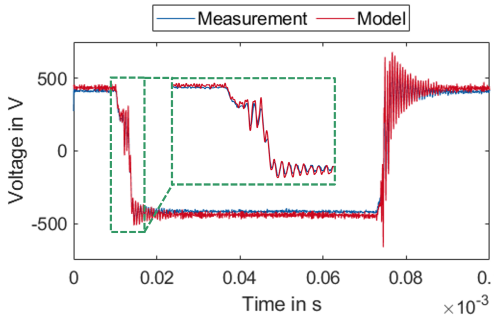

(a)

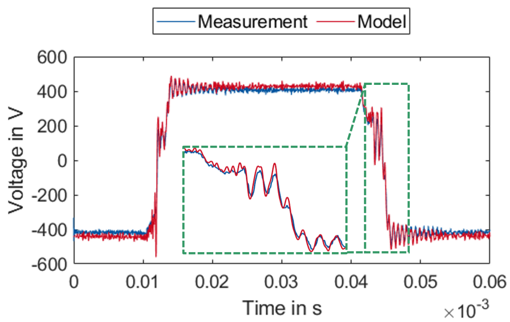

(b)

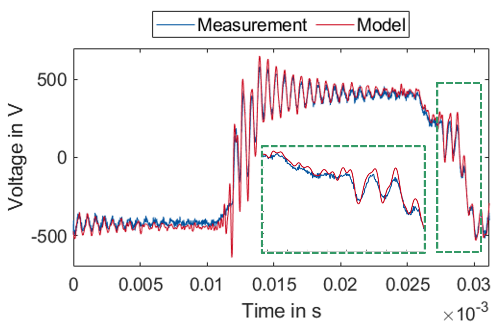

(c)

Fig. 7. Representative comparison of measured and modeled common-mode voltage at the IPMSM terminals in time-domain validation: (a)$f_{\mathbf{sw}} = 8\,\mathrm{kHz}$ $n = 500$ rpm, (b)$f_{\mathbf{sw}} = 16\,\mathrm{kHz}$ $n = 1000$ rpm, (c)$f_{\mathbf{sw}} = 32\,\mathrm{kHz}$ $n = 2000$ rpm,

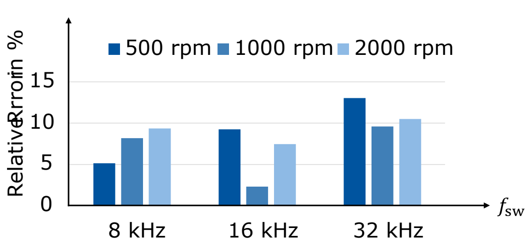

Fig. 8. Statistics of the relative error between modeled and measured CM peak voltage at the IPMSM terminals under various switching frequencies $f_{\mathbf{sw}}$ and operating speeds n.

tions. An average error of 8.31 % is achieved in predicting the common-mode voltage peak during switching operations across switching frequencies ranging from 8 kHz to 32 kHz. These results confirm the model's broad applicability in simulating switching-induced transient behaviors across different machine and winding types. The proposed model is a reliable tool for analyzing voltage stress and optimizing insulation system design in electric drive systems, particularly those incorporating WBG power devices and long power cables. Future work will focus on extending its capabilities to predict bearing current in electric machines during the switching processes of power converters.

References

[1] M. F. Rahman, P. Niknejad, and M. R. Barzegaran, "Comparing the performance of si igbt and sic mosfet switches in modular multilevel converters for medium voltage pmsm speed control," in *2018 IEEE Texas Power and Energy Conference (TPEC)*, 2018, pp. 1–6.

[2] M. Buffolo, D. Favero, A. Marcuzzi, C. D. Santi, G. Meneghesso, E. Zanoni, and M. Meneghini, "Review and outlook on gan and sic power devices: Industrial state-of-the-art, applications, and perspectives," *IEEE Transactions on Electron Devices*, vol. 71, no. 3, pp. 1344–1355, 2024.

[3] M. Sadoughi, F. Fateh, and B. Mirafzal, "Overvoltage stress on ac motor winding insulations driven by fast-switching inverters: A study," in *2024 IEEE Kansas Power and Energy Conference (KPEC)*, 2024, pp. 1–6.

[4] International Electrotechnical Commission (IEC), "Iec 60034-18-41: Rotating electrical machines - part 18-41: Functional evaluation of insulation systems - test procedures for voltage endurance of insulation systems," 2014.

[5] Y. Ryu, M. Yea, J. Kim, and K. J. Han, "Stator impedance modeling platform for the electromagnetic compatibility aware design of 3.7- to 7.5-kw squirrel-cage induction motors," *IEEE Transactions on Industrial Electronics*, vol. 68, no. 11, pp. 11 255–11 265, Nov. 2021.

[6] J. E. Ruiz-Sarrio, F. Chauvicourt, J. Gyselinck, and C. Martis, "Impedance modeling oriented toward the early prediction of high-frequency response for permanent magnet synchronous machines," *IEEE Transactions on Industrial Electronics*, vol. 70, no. 5, pp. 4548–4557, May 2023.

[7] S. Dong, D. Zhang, and T. Fan, "High frequency model of six-phase open-winding motor for emi analysis," in *2022 25th International Conference on Electrical Machines and Systems (ICEMS)*, 2022, pp. 1–5.

[8] A. Hoffmann and B. Ponick, "Statistical deviation of high-frequency lumped model parameters for stator windings in three-phase electrical machines," in *2020 International Symposium on Power Electronics, Electrical Drives, Automation and Motion (SPEEDAM)*, 2020, pp. 85–90.

[9] H. Peng, Z. Luo, Y. Yu, and K. Hameyer, "Modeling voltage distribution along the hairpin windings of an electrical machine using impedance fitting," in *2024 International Conference on Electrical Machines (ICEM)*, 2024, pp. 1–7.

[10] H. Peng, N. Driendl, S. Stevic, D. Butterweck, Y. Firouz, L. Sharifian, and K. Hameyer, "High-frequency modeling of permanent magnet synchronous machines using grey box models," *IEEE Transactions on Transportation Electrification*, vol. 10, no. 4, pp. 8150–8160, 2024.

[11] R. J. Allemang, R. S. Patwardhan, M. M. Kolluri, and A. W. Phillips, "Frequency response function estimation techniques and the corresponding coherence functions: A review and update," in *Mechanical Systems and Signal Processing*, vol. 162, 2022, p. 108100. [Online]. Available: https://www.sciencedirect.com/science/article/pii/S0888327021004830